Doctoral Dissertation (Censored)

博士論文(要約)

Evaluation of Telomerase Reverse Transcriptase Localization during Cell Death Process by Live-Cell Imaging

(生細胞イメージングを用いた細胞死過程における テロメラーゼ逆転写酵素 TERT の局在評価)

A Dissertation Submitted for the Degree of Doctor of Philosophy

December 2021

令和 3 年 12 月博士(理学)申請

Department of Biological Sciences, Graduate School of Science,

The University of Tokyo

東京大学大学院理学系研究科生物科学専攻

Hiroshi Ebata

江端拓志

Abstract

Telomerase reverse transcriptase (TERT) is a protein subunit of telomerase complex and elongates telomeres by reverse transcription. In human, TERT is highly expressed in most cancer cells and the telomere elongation by TERT is considered to enable cancer cells to proliferate indefinitely. Besides its canonical telomere elongation function, TERT is also expected to play a noncanonical role because it localizes not only in nuclear but also in mitochondria, which lack telomeres. Mitochondria involves in various biological phenomena including cancer homeostasis, and thus, I speculate that mitochondrial TERT plays important roles, which have been thought to be achieved by telomere elongation in cancer regulation. Several studies have found that TERT accumulates to mitochondria after oxidative stress and controls apoptosis induced by oxidative stress. However, there remains controversy about whether mitochondrial TERT induces or suppresses apoptosis. I assume that this controversy results from the lack of spatiotemporal information for TERT distribution and cell death in individual cells. In response, here I simultaneously detected apoptosis and TERT localization after oxidative stress in individual HeLa cells by live-cell tracking. This tracking revealed that the oxidative stress-induced increase of mitochondrial TERT triggered apoptosis but the increase positively correlated with the time until cell death. The results propose a new model in which mitochondrial TERT has two opposing effects at different stages of apoptosis: it predetermines apoptosis at the first stage of cell-fate determination but also delays apoptosis at the second stage. These distinct effects respectively support both sides of the controversy about the role

of mitochondrial TERT in apoptosis, and thus, my model integrates two opposing hypotheses. Furthermore, detailed statistical analysis of TERT mutations, which have been predicted to inhibit TERT transport to mitochondria, revealed that these mutations suppress apoptosis independent of the mitochondrial localization of TERT. Altogether, these results indicate that mitochondrial TERT involves in apoptosis through several different noncanonical functions.

List of Abbreviations

In alphabetical order

Abbreviation	Full name
BCL-2	B cell lymphoma-2
BCL-xL	B cell lymphoma-extra large
bp	base pair
BSA	bovine serum albumin
CCD	charge-coupled device
CRISPR	clustered regularly interspaced short palindromic repeats
CTE	C-terminal extension
Cas9	CRISPR-associated protein 9
DMEM	Dulbecco's modified Eagle medium
DNA	deoxyribonucleic acid
GFP	green fluorescent protein
gRNA	guide RNA
HA	homology arm
HEK293T	human embryonic kidney 293T
IFD-TRAP	insertions in the finger domain-trapping telomerase RNA

KDE	kernel density estimation
LED	light emitting diode
MCC	Manders' colocalization coefficient
MCL-1	myeloid cell leukemia-1
miRNA	microRNA
MMP	mitochondrial membrane potential
MOMP	mitochondrial outer membrane permeabilization
MTS	mitochondrial targeting signal
NADH	nicotinamide adenine dinucleotide hydrogen
ND1/2	NADH-ubiquinone oxidoreductase chain 1/2
NES	nuclear export signal
NF-κB	nuclear factor-κB
NLS	nuclear localization signal
PBS	Phosphate-buffered saline
PCC	Pearson's correlation coefficient
PCR	polymerase chain reaction
PVDF	polyvinylidene fluoride
PenStrep	penicillin-streptomycin

qPCR	quantitative PCR
RNA	ribonucleic acid
RT	reverse transcriptase domain
RdRP	RNA-dependent RNA polymerase
SEM	standard error of the mean
siRNA	small interfering RNA
TEN	telomerase essential N-terminal domain
TERC / TR	telomerase RNA component
TERT	telomerase reverse transcriptase
TRAP	telomeric repeat amplification protocol
TRBD	telomerase RNA binding domain
WT	wild-type
Z-VAD-fmk	N-benzyloxycarbonyl-Valyl-Alanyl-Aspartyl-fluoromethylketone
ZFN	zinc finger nuclease

TABLE OF CONTENTS

LIST OF FIGURES AND TABLES

CHAPTER 1

INTRODUCTION

In eukaryotic cells, exposed chromosomal ends are recognized as double-strand breaks and are targeted by DNA repair system, resulting in abnormal connections of chromosomes. To prevent this misrecognition, original chromosomal ends have repetitive DNA sequences called telomeric regions. This repetitive sequence is G-rich (TTAGGG repeats in humans) and forms G-quadruplex conformation. G-quadruplex itself has protective role for chromosomal ends [1] and recruits protein complex called shelterin, which strengthens the protection [2]. However, since telomeric regions locate at the chromosomal ends, these regions are used as scaffolds for primers in DNA replication and shorten at every cell division. When the length of telomere reaches a certain length, G-quadruplex cannot be formed, and chromosomal ends are exposed and repaired abnormally. This wrong repair stops cell division and results in senescence or apoptosis [3] (Fig. 1.1).

Telomerase was found as an enzyme, which elongates the telomeric repeat sequences and prevents telomere loss [4]. Among the ribonucleoprotein complex of telomerase, telomerase reverse transcriptase (TERT) is a protein subunit, which executes reverse transcription of telomeres and directly repairs them [5]. TERT binds to RNA template of telomeres, telomerase RNA component (TERC or TR) and *in vitro* study has revealed that these two components are sufficient to demonstrate telomerase activity [6]. In humans, most cancer cells express high levels of TERT,

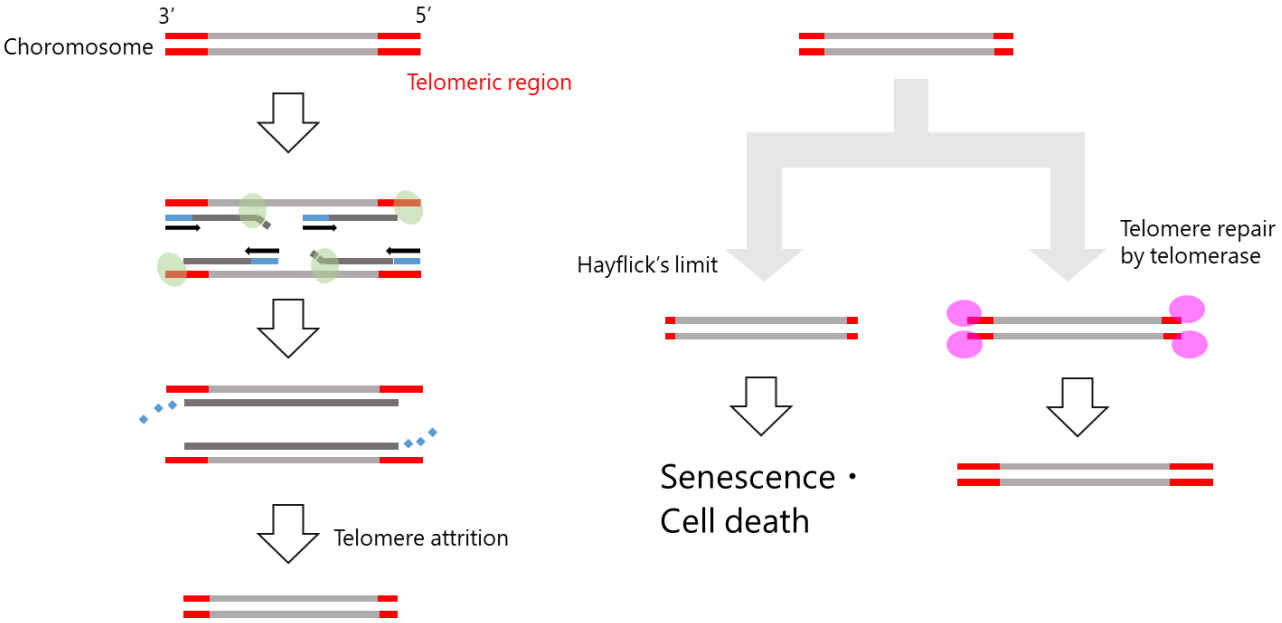

Figure 1.1 Canonical function of telomerase to overcome the end-replication problem.

whereas somatic cells suppress TERT expression [7]. On the contrary, TERC is expressed almost all the cells irrelevant to cancerous property of cells [8]. Since TERT enables cells to proliferate indefinitely, it is believed to promote the unlimited growth of cancer cells.

The unique characteristic of TERT that human somatic cells suppress its expression has made researchers consider TERT as an ideal target for cancer therapy, because suppressing TERT expression would not harm somatic cells and would not cause serious side effects. Through numerous studies of functional sequence analysis on TERT, TERT has been reported to have several domains and localization signal sequences including nuclear localization signal (NLS) [9], nuclear export signal (NES) [10, 11], and mitochondrial targeting signal (MTS) [12] (Fig. 1.2). As the existence of these signals suggests, many studies have shown that TERT localized not only in the nucleus but also in cytoplasm and mitochondria [12, 13, 14, 15, 16, 17, 18, 19]. Molecular mechanisms that facilitate the translocation of TERT between nuclear and cytoplasm has been elucidated. Nuclear import of TERT is regulated by kinase Akt [9, 20, 21, 22], NF-κB [21, 23], and 14-3-3 protein [11, 21], while export of TERT from nuclear is dependent on nuclear exportin CRM1 [11, 13], Src kinase [13], and Shp2 [24]. These strict regulations of TERT localization are considered to relate to noncanonical transcriptional regulations by nuclear TERT. Telomere length-independent activities of TERT have been reported to regulate transcription by Myc, which promoted cell proliferation and lymphomagenesis [25, 26], by Wnt/β-catenin, which promoted cell proliferation and embryonic

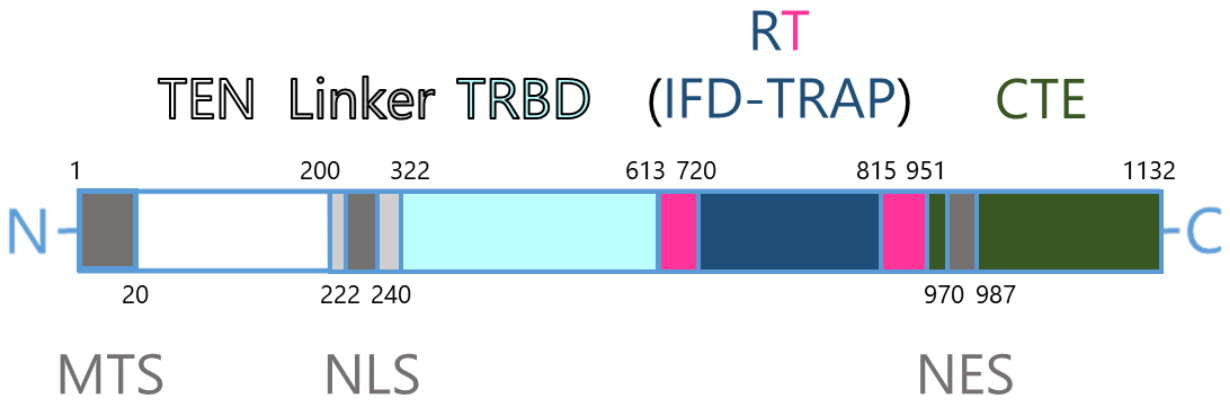

Figure 1.2 Domain structure of human TERT

MTS, mitochondrial targeting signal; TEN, telomerase essential N-terminal domain; NLS, nuclear localization signal; TRBD, telomerase RNA binding domain; RT, reverse transcriptase domain; IFD-TRAP, insertions in the finger domain-trapping telomerase RNA; CTE, C-terminal extension; NES, nuclear export signal.

development [25, 27], and by NF-κB pathway, which increased gene expression related to inflammation and cancer progression [28]. In addition, TERT has been found to have RNA-dependent RNA polymerase (RdRP) activity to produce siRNA targeting heterochromatic regions and promoted heterochromatin assembly and mitotic progression [29], leading to the regulation of DNA damage response [30]. TERT has also been reported to regulate dozens of miRNA levels [31]. Besides the canonical telomere elongation function, these noncanonical gene expression regulations by nuclear TERT have also been considered to regulate cancer cell progressions.

Although the pathway of TERT translocation between nuclear and cytoplasm has been well established, only little is known about mitochondrial transport of TERT and mitochondrial TERT function. Unlike linear chromosome, mitochondrial DNA is circular and lacks telomeric regions. In addition, TERC, the template RNA component of telomerase, does not localize to mitochondria [33]. These findings lead to the assumption that mitochondrial TERT also has a noncanonical role beyond its telomere elongation function. Several studies reported that oxidative stress increases TERT localization in mitochondria [16, 18] and mitochondrial accumulation of TERT prevents mitochondrial DNA damage and production of reactive oxygen species (ROS) induced by oxidative stress [17, 18, 32, 33, 34, 35, 36, 37, 38]. The mitochondrial accumulation of TERT is dependent on the nuclear export regulation by Src kinase [13], but it remains unclear what molecular mechanisms regulate mitochondrial TERT transport from cytoplasm and TERT functions of mitochondrial DNA

protection and ROS reduction. Mitochondrial DNA protection and ROS reduction rely on reverse transcriptase activity of TERT, even though mitochondrial TERT does not interact with TERC [33]. Thus, the noncanonical functions of mitochondrial TERT is likely to relate to nucleotide regulation of TERT. TERT localizes to matrix in mitochondria and binds to mitochondrial DNA at the coding regions for the NADH-ubiquinone oxidoreductase chain 1 (ND1) and ND2 [32, 33]. Also, similar to nuclear TERT, mitochondrial TERT shows RdRP activity to produce siRNAs from the RNA component of mitochondrial RNA processing endoribonuclease in a Dicer-dependent manner [39], and siRNAs from chemical synthesized RNA in a Dicer-independent manner [40]. These nucleotide-related activity of mitochondrial TERT can be responsible for TERT functions in mitochondria.

Oxidative stress causes apoptosis besides mitochondrial DNA damage and ROS production, and mitochondrial TERT has reported to regulate apoptosis. Apoptosis is divided into two types, intrinsic apoptosis and extrinsic apoptosis [41]. Both types of apoptosis are interconnected, but in general, intrinsic apoptosis is mitochondria-mediated and induced by low concentration of oxidative stress [42, 43]. In intrinsic apoptosis, pro-apoptotic BCL-2 family proteins are recruited to outer mitochondrial membrane and form pores on the membrane. This pore formation leads to mitochondrial outer membrane permeabilization (MOMP) to facilitate cytochrome c release, which activates apoptosis executioner caspase. Cancer cells downregulate pro-apoptotic proteins and upregulate anti-apoptotic BCL-2 family proteins, which bind to the pro-apoptotic proteins and inhibit

its pore formation. TERT has been reported to have a conserved motif among BCL-2 family proteins and to interact with the anti-apoptotic BCL-2 family proteins BCL-xL and MCL-1 via the motif [44]. However, the effect of mitochondrial TERT interaction with BCL-xL and MCL-1 is elusive. Moreover, the effect of mitochondrial TERT itself on apoptosis has been controversial. Mutagenesis studies for MTS or target residue of Src kinase that is responsible to export TERT from nuclear by oxidative stress have proposed that mitochondrial TERT induces apoptosis [13, 16]. However, TERT overexpression has been reported to increase TERT in mitochondria and cell survival after oxidative stress, suggesting that mitochondrial TERT suppresses apoptosis [18, 19, 35]. These reports, while conflicting, have shed light on the possibility that mitochondrial TERT regulates apoptosis.

These conflicting observations can be attributed mainly to three reasons. First, the relationship between TERT localization and cell death in individual cells has not been fully tested. Because fluorescently labeled TERT fails to retain normal TERT enzymatic activity and cellular distribution, previous studies have detected mitochondrial TERT only after cell fixation or cell disruption [13, 16, 18]. Therefore, the eventual fate of each individual cell used in the studies is unknown. Secondly, temporal information on cell death and TERT distribution is limited. Previous immunofluorescence- and flow cytometry-based measurements of cell death only provide information on cell death and TERT localization at a specific time. However, the response time to apoptosis-inducing stimuli varies among cells. Moreover, oxidative stress induces cell death through several

different pathways [42, 43, 45]. Thus, to directly test the relationship between mitochondrial TERT and apoptosis, temporally tracking the two factors is required. Thirdly, traditional experimental procedures can hurt the cells. For example, immunocytochemistry needs plenty of washes for each step of fixation, permeabilization, and antibody binding. Cells experiencing cell death are no longer adhesive to the dish surface and some disappear by the washes. The loss of dead cells results in underrating apoptosis. In flow cytometry cell death measurements, flowing cells experience various physical stresses, such as high pressures, shear forces, electrical charges, shock forces, and rapid temperature changes. These excessive stresses can promote stress responses in the cells, resulting in overestimating cell death. Therefore, to directly test the relationship between mitochondrial TERT localization and cell death, stress-free methods for cell death detection is necessary.

In response, here I combined an imaging-based dead-cell detection method with fluorescence live-cell imaging of TERT to directly evaluate the association between the mitochondrial TERT localization and apoptosis of individual cells. Live-cell imaging provides spatiotemporal information of the TERT localization until apoptosis. This method has several advantages over classical dead-cell detection methods. Especially, live-cell imaging keeps away from additional physical stresses to the cells because it needs only one medium exchange to induce oxidative stress without any washing steps. Also, to visualize TERT localization in an individual cell, I inserted a fluorescent protein, mVenus, to TERT at a position that did not impede the mitochondrial

TERT localization or enzymatic activity. This setup enabled us to track the temporal changes of TERT localization. Accordingly, I found that the mitochondrial accumulation of TERT occurred immediately after oxidative stress in a subset of cells to trigger apoptosis but, at the same time, the accumulation positively correlated with time until apoptosis. These results propose that mitochondrial TERT plays distinct roles at different stages of apoptosis. I also unraveled the effects of previously reported TERT mutations and found that their inhibition influences on apoptosis are independent of mitochondrial TERT localization.

CHAPTER 2

METHODS

Plasmids

For generation of stable cell line, the gene encoding TERT was amplified from the plasmid pCDH-3xFLAG-TERT, which was distributed from Steven Artandi (Addgene plasmid # 51631 ; http://n2t.net/addgene:51631). The mVenus sequence was isolated from pCS2-mVenus plasmid, which was purchased from the RIKEN BioResorce Research Center (RDB15116, Ibaraki, Japan). pSBbi-Pur was distributed from Eric Kowarz (Addgene plasmid # 60523 ; http://n2t.net/addgene:60523). The gene encoding TERT and mVenus was inserted into pSBbi vector using the In-Fusion cloning kit (Takara Bio, Shiga, Japan). The R3E/R6E mutation was introduced using the KOD mutagenesis kit (Toyobo, Osaka, Japan). The Y707F mutation was introduced by PCR (primers are listed in Table 2.1 and 2.2).

For genome editing, the donor template was created from the FLAG-LoxP-GFP-LoxP-SNAP-TERT, which was distributed from Thomas Cech (Addgene plasmid # 71391 ; http://n2t.net/addgene:71391). The FLAG-LoxP-GFP-LoxP-SNAP-TERT contained homology arms, which were 1062 bp upstream of the target site and 996 bp downstream of the target site in *TERT* locus. The LoxP-GFP-LoxP sequence was isolated from the FLAG-LoxP-GFP-LoxP-SNAP-TERT plasmid. To make frame shift for conditional knockout, 1 nucleotide between GFP and loxP

was deleted by PCR. As Cas9 D10A-gRNA expression vector, All-in-One NickaseNinja vector was purchased from ATUM (Newark, CA USA). gRNAs were designed at Crispr.mit.Edu to target 132 bp downstream of the target site and 177 bp downstream of the target site. The DNA sequences for gRNAs were synthesized as complementary forward and reverse primers from Eurofins. Then, the primers were mixed and annealed by gradually decreasing temperature from 95° C to 4° C on a thermal cycler. Using the In-Fusion cloning kit, the GFP sequence was inserted into homology arms from the FLAG-LoxP-GFP-LoxP-SNAP-TERT plasmid, and the gRNAs were inserted into the All-in-One NickaseNinja vector.

All plasmids were transformed into DH5α chemical competent cells and purified using the FastGene miniprep kit and endotoxin-free miniprep kit (NIPPON Genetics, Tokyo, Japan). The primer sets used are presented in Table 2.1 and 2.2.

Cell culture and generation of stable cell line

The HeLa cell line and the HEK293T cell line were purchased from RIKEN BioResource Research Center (RCB0007 and RCB2202, respectively). All cells were cultured in DMEM supplemented with 10% FBS and 1 × PenStrep in a 6-well plate at 37° C, 5% CO_2. Cells in 6-well plates were transfected with 1.9 μg of pSBbi-TERT-Pur plasmid, 0.1 μg of pCMV-SB100 [46] and 3.75 μg of PEI in 250 μL of Opti-MEM. After transfection, cells were selected in DMEM supplemented with 10% FBS, 1 × PenStrep, and 1 μg/mL Puromycin for one week.

Table 2.1 Key PCR primers to generate the insertion part of TERT constructs used in this study.

Construct	PCR Template	PCR Primer
TERT	pCDH-3xFLAG-TERT	5′-AAACTACCCCAAGCTGGCCTCTGAGGCCATGC-3′ 5′-TTGATCCCCAAGCTTGGCCTGACAGGCCTCAG-3′
mVenus	pCS2-mVenus	5′-ATGGTGAGCAAGGGCGAGG-3′ 5′-CTTGTACAGCTCGTCCATGCCG-3′
pSBbi-TERT R3E/R6E-Pur	pSBbi-TERT-Pur	5′-CCCGAGTGCCGAGCCGTGCGCTCCCTG-3′ 5′-AGCCTCCGGCATGGCCTCAGAGGCCTTTCGA-3′
pSBbi-TERT Y707F-Pur	pSBbi-TERT-Pur	5′-TTTGTCAAGGTGGATGTGACGG-3′ 5′-GAACAGCTCAGGCGGCG-3′
pSBbi-mVenus-TERT R3E/R6E-Pur	pSBbi-mVenus-TERT-Pur	5′-CCCGAGTGCCGAGCCGTGCGCTCCCTG-3′ 5′-AGCCTCCGGCATGGCCTCAGAGGCCTTTCGA-3′
pSBbi-mVenus-TERT Y707F-Pur	pSBbi-mVenus-TERT-Pur	5′-TTTGTCAAGGTGGATGTGACGG-3′ 5′-GAACAGCTCAGGCGGCG-3′
LoxP-GFP-LoxP	FLAG-LoxP-GFP-LoxP-SNAP-TERT	5′-GCCACCCCCGCGATGATAACTTCGTATAATGTAT GTATGCTATACGAAGTTATAAGCTTTG-3′ 5′-GGCTAGCGGCAGCACGGTACCGGATAACTTCGTA TAGCATAC-3′
LoxP-GFP-LoxP-TERT (1 nt deletion)	LoxP-GFP-LoxP-TERT	5′-ATAAAATATCTTTATTTTCATTACATCTGTGTGT TGG-3′ 5′-CTTGTACAGCTCGTCCATGCCG-3′

Table 2.2 Key PCR primers to generate the vector part of TERT constructs used in this study.

Construct	PCR Template	PCR Primers	Inserts
pSBbi-TERT-Pur	pSBbi-Pur	5′-AAGCTTGGGGATCAATTCTCTAGAG-3′ 5′-AGCTTGGGGTAGTTTTCACGAC-3′	TERT
pSBbi-mVenus-TERT-Pur (A67-A68)	pSBbi-TERT-Pur	5′-GACGAGCTGTACAAGGCCCCCTCCTTCCGCCA-3′ 5′-GCCCTTGCTCACCATGGCGGGGGGCGGCCGT-3′	mVenus
pSBbi-TERT-mVenus-Pur (Cter)	pSBbi-TERT-Pur	5′-GACGAGCTGTACAAGTGAGGCCTGTCAGGCC-3′ 5′-CTCGCCCTTGCTCACCCCCGGACCCGGACCGTCCAGGATGGTCTTGAAGTCTG-3′	mVenus
LoxP-GFP-LoxP-TERT	FLAG-LoxP-GFP-LoxP-SNAP-TERT	5′-GCGCTCCCC-3′ 5′-CATCGCGGGGGTGGC-3′	LoxP-GFP-LoxP

Immunofluorescence

Two days before immunofluorescence, cells were passaged in a black wall poly-L-lysine-coated multi-well glass bottom dish (Matsunami, Osaka, Japan) at a density of 4000 cells per well. The cells were incubated with DMEM supplemented with 10% FBS, 1 × PenStrep, and 100 nM MitoTracker Deep Red FM (Thermo Fisher Scientific, Waltham, MA USA) for 30 min at 37° C, 5% CO_2. All procedures after incubation with MitoTracker Deep Red FM were performed under room temperature in the dark. The washing step referred to exchange the medium for PBS and to incubate the cells for 5 min.

Fixation was performed using 4% paraformaldehyde in PBS (Nacalai, Kyoto, Japan) for 10 min followed by washing. Permeabilization was performed with 0.5% Triton-X-100 in PBS for 10 min followed by 3 washes. Blocking was performed with 3% BSA in PBS-T for 1 hour followed by washing.

For immunofluorescence with the TERT mutations, the cells were incubated with 20 μM Cellstain Hoechst 33342 (Wako, Osaka, Japan) in PBS for 10 min and washed. The cells were then incubated with 1:500 diluted anti-TERT antibody (Rockland, Limerick, PA USA, 600-401-252S) in PBS-T for 1 hour and washed 3 times. Finally, the cells were incubated with 1:2000 diluted anti-rabbit IgG (H+L), F(ab')2 Fragment conjugated with Alexa Fluor 488 (CST, Danvers, MA USA) in PBS-T for 1 hour and washed 3 times.

For the immunofluorescence of cells expressing mVenus-TERT, after blocking, the cells were washed 3 times and then incubated with anti-TERT antibody conjugated with CF405M (1:100 dilution) in PBS-T for 1 hour and washed 3 times. Dye conjugation was performed using the Mix-n-Stain CF405M Antibody Labeling Kit (Biotium, Fremont, CA USA). Anti-TERT antibody conjugated with CF405M was diluted at 1:5 in storage buffer.

The imaging medium for immunofluorescence was PBS supplemented with 1% ProLong Live Antifade Reagent (Thermo Fisher Scientific).

Immunofluorescence imaging of the cells was performed using a SpinSR10 (Olympus, Tokyo, Japan) with an oil-immersion objective (PlanApoN 60×/1.40 Oil, Olympus). Fluorophores were excited at 405 nm (for Hoechst or CF405M), 488 nm (for Alexa Fluor 488), 512 nm (for mVenus), and 640 nm (for MitoTracker Deep Red FM) lasers.

Knock-in of mVenus to *TERT* locus with CRISPR/Cas9 system

Cells in 6 cm dishes were transfected with 2.8 μg of LoxP-EGFP-LoxP-TERT donor template, 1.4 μg each of All-in-One NickaseNinja vector carrying gRNA, 7.5 μL of Lipofectamine 3000 (Thermo Fisher Scientific), and 10 μL of P3000 (ThermoFisher) in 500 μL of Opti-MEM. Transfected cells were cultured for 2 weeks and sorted into 12 well plate by GFP signal in flow-cytometry by BD FACSAria III (BD Biosciences) or On-chip Sort (On-chip Biotechnologies). Sorted cells were passaged to 96 well plate as 0.5 cells/well. After 3-4 weeks, cells were harvested and knock-in was

evaluated by colony PCR.

Dead cell detection with live-cell imaging

Cells were cultivated for a week before the assay and passaged 5 times. A day before the assay, the cells were passaged into black wall poly-L coated 96-well plates at a density of 1000 cells per well. All empty wells and space between wells were filled with sterilized water.

Cells were treated with DMEM supplemented with 10% FBS, 1 × PenStrep, and 267 μM sodium carbonate hydrogen peroxide (equivalent to 267 μM sodium carbonate and 400 μM hydrogen peroxide) for 3 hours. As negative controls, cells were treated with DMEM supplemented with 10% FBS, 1 × PenStrep, and 267 μM sodium carbonate. During imaging, all cells were cultured in DMEM supplemented with 10% FBS, 1 × PenStrep, 250 nM SYTOX Orange (Thermo Fisher Scientific) and 2.5 μM YO-PRO-1 (Thermo Fisher Scientific) at 37° C and 5% CO_2.

For live-cell imaging with Z-VAD-fmk, the cells were treated with DMEM supplemented with 10% FBS, 1 × PenStrep, 50 μM Z-VAD-fmk (InvivoGen, San Diego, CA USA), and 267 μM sodium carbonate hydrogen peroxide for 3 hours. Then, the cells were cultured in DMEM supplemented with 10% FBS, 1 × PenStrep, 50 μM Z-VAD-fmk, 250 nM SYTOX Orange (Thermo Fisher Scientific) and 2.5 μM YO-PRO-1 (Thermo Fisher Scientific) at 37° C and 5% CO_2.

Telomerase activity assay

5.0 × 10^6 cells were harvested and frozen at -80° C. Thawed cells were treated with and assayed following the instructions of the Telomerase Activity Quantification qPCR Assay Kit (ScienCell, Carlsbad, CA USA). qPCR was performed using OneStepPlus (Thermo Fisher Scientific).

An assay to measure telomerase activity has been established as telomeric repeat amplification protocol (TRAP) assay [47]. In this assay telomerase in cell lysates extends the telomerase substrate by adding telomere repeats. Then, the products are amplified by PCR using specific primers. Conventional TRAP assay detects the amplified products by electrophoresis, but in the kit here, amplification step and detection step are unified as qPCR.

Western blotting

10 μg of whole cell lysates prepared in telomerase activity assay was loaded on to a 4–15% precast polyacrylamide gel (Bio-Rad, Hercules, CA USA). The protein concentration of each lysate was measured using a Pierce 660 nm Protein Assay Kit (Thermo Fisher Scientific) with NanoDrop 2000c (Thermo Fisher Scientific). Proteins were transferred into a PVDF membrane using the Trans-Blot Turbo Transfer System (Bio-Rad), and the transferred membrane was blotted using the iBind Western System (Thermo Fisher Scientific). The primary antibodies used were anti-TERT antibody (dilution 1:200; Rockland) and anti-β tubulin antibody (dilution 1:200; CST). IgG Detector Solution v2 from Western BloT Rapid v2 (Takara Bio) was employed as the secondary antibody at a dilution of

1:1000. SuperSignal West Femto Maximum Sensitivity Substrate (Thermo Fisher Scientific) and ImmunoStar Basic (Wako) were used as substrates for horseradish peroxidase. Protein bands were detected using an ImageQuant LAS4000 mini (GE Healthcare, Chicago, IL USA), and the intensities were measured using the Gel tool of Fiji/ImageJ [48, 49].

Dead cell detection and TERT visualization by live-cell tracking

Cells were cultivated a week before the assay and passaged 5 times. A day before the assay, the cells were passaged into black wall poly-L-lysine coated 96-well plates at a density of 1000 cells per well. All empty wells and space between wells were filled with sterilized water. Cells were incubated with DMEM supplemented with 10% FBS, 1 × PenStrep, and 100 nM MitoTracker Deep Red FM for 30 min at 37° C and 5% CO_2. For the oxidative stress, the cells were treated with DMEM supplemented with 10% FBS, 1 × PenStrep, and 267 μM sodium carbonate hydrogen peroxide (equivalent to 267 μM sodium carbonate and 400 μM hydrogen peroxide) for 3 hours. As negative controls, cells were treated with DMEM supplemented with 10% FBS, 1 × PenStrep, and 267 μM sodium carbonate. During imaging, all cells were cultured in DMEM supplemented with 10% FBS, 1 × PenStrep and 250 nM SYTOX Blue (Thermo Fisher Scientific) at 37° C and 5% CO_2.

For control experiments with Hoechst, cells were incubated with 10% FBS, 1 × PenStrep, and 100 nM MitoTracker Deep Red FM (Thermo Fisher Scientific) for 30 min at 37° C and 5% CO_2, and then were incubated with 10% FBS, 1 × PenStrep, and 20 μM Cellstain Hoechst 33342 (Wako)

for 15 min at 37° C and 5% CO_2.

Microscopy for live-cell imaging and tracking

Imaging was performed using an inverted microscope (Ti, Nikon, Tokyo, Japan) with an objective (Plan Apo Lambda 40×/0.95, Nikon), LED illumination system (X-Cite XLED1, Lumen Dynamics, Ontario, Canada) and filter sets [CFP-2432C (for SYTOX-Blue or Cellstain Hoechst 33342; Semrock), GFP-3035D (for YO-PRO-1; Semrock), LF514-B (for mVenus; Semrock), TRITC-A-Basic (for SYTOX-Orange; Semrock), and Cy5-4040C (for MitoTracker Deep Red FM; Semrock)]. Bright-field and fluorescence images were captured using an electron multiplying CCD camera (ImagEM X2-1K EM-CCD, Hamamatsu Photonics, Shizuoka, Japan). The sample temperature was kept at 37° C by feedback from a heat sensor in a water-filled well and was monitored by NECO (TOKAI HIT, Shizuoka, Japan).

For the live-cell imaging, dead cells were defined as cells that were stained with SYTOX Orange or YO-PRO-1; the threshold was set to the mean intensity of negative control cells plus 10 times of the standard deviation using NIS-Elements software (Nikon).

For live-cell tracking, a 1.5× magnification lens was added to the system, and dead cells were defined as cells that were stained with SYTOX Blue; the threshold was set to the mean intensity of negative control cells plus 5 times of the standard deviation using NIS-Elements software.

For control experiments with Hoechst, dead cells were defined as cells that were stained with SYTOX Orange; the threshold was set to the mean intensity of negative control cells plus 10 times the standard deviation using NIS-Elements software.

Colocalization analysis

A bright field image in each timeframe was used to set regions of cells, which were used as regions of interest for further analysis. Otsu's method [50] was employed to find pixels above a certain fluorescence threshold, and Manders' colocalization coefficients (MCCs) were calculated in the pixels using the GDSC colocalization plugins for Fiji/ImageJ [51].

MCC of TERT with mitochondria was calculated from TERT intensity T and mitochondria intensity M as:

$$\mathrm{MCC} = \frac{\sum_i T_{i,colocal}}{\sum_i T_i}$$

where $T_{i,colocal} = T_i$ if $M_i > 0$ and $T_{i,colocal} = 0$ if $M_i = 0$.

Statistical analysis

Statistical tests were performed using R software [52] or OASIS2 [53]. The Steel-Dwass test was performed using the NSM3 library with the Monte Carlo method [54]. The log-rank test was performed for groups containing all datasets from independent experiments.

CHAPTER 3

RESULTS

CRISPR/Cas9 based homozygous knock-in to *TERT* locus is lethal in cancer cells

In preparation for TERT localization study by introducing exogenous TERT with mutations, I planned to execute knockout of endogenous *TERT*. For cell culture, TERT serves as an immortalization factor and thus, knockout of *TERT* has resulted in growth retardation and susceptibility to apoptosis in several studies [55, 56]. Without cell sorting, unaffected cells outgrow *TERT*-knockout cells and it is difficult to clone *TERT*-knockout cells. In contrast, unaffected cells cause apoptosis by excessive stress from cell sorting. Therefore, conditional knockout of *TERT* is suitable for my aim to generate stable cell lines without endogenous TERT expression. In a previous study, CRISPR/Cas9-based knock-in of tags, fluorescent proteins, and target sites for Cre recombinase to *TERT* locus has been established [57]. I assumed that it is useful to knock-in target sites for Cre recombinase and fluorescent protein to achieve conditional knockout and cell sorting, respectively (Fig. 3.1). Here, I designed conditional knockout workflow for HeLa and HEK293T cells.

First, I designed donor template and gRNAs for knock-in of LoxP-SV40-GFP-LoxP sequence into TERT by Cas9 D10A (Fig. 3.1). I transfected these plasmids into HeLa cells and sorted the cells 3 times in flow-cytometry by fluorescence intensity of GFP (Fig. 3.2.A). As the sorting proceeded, cell

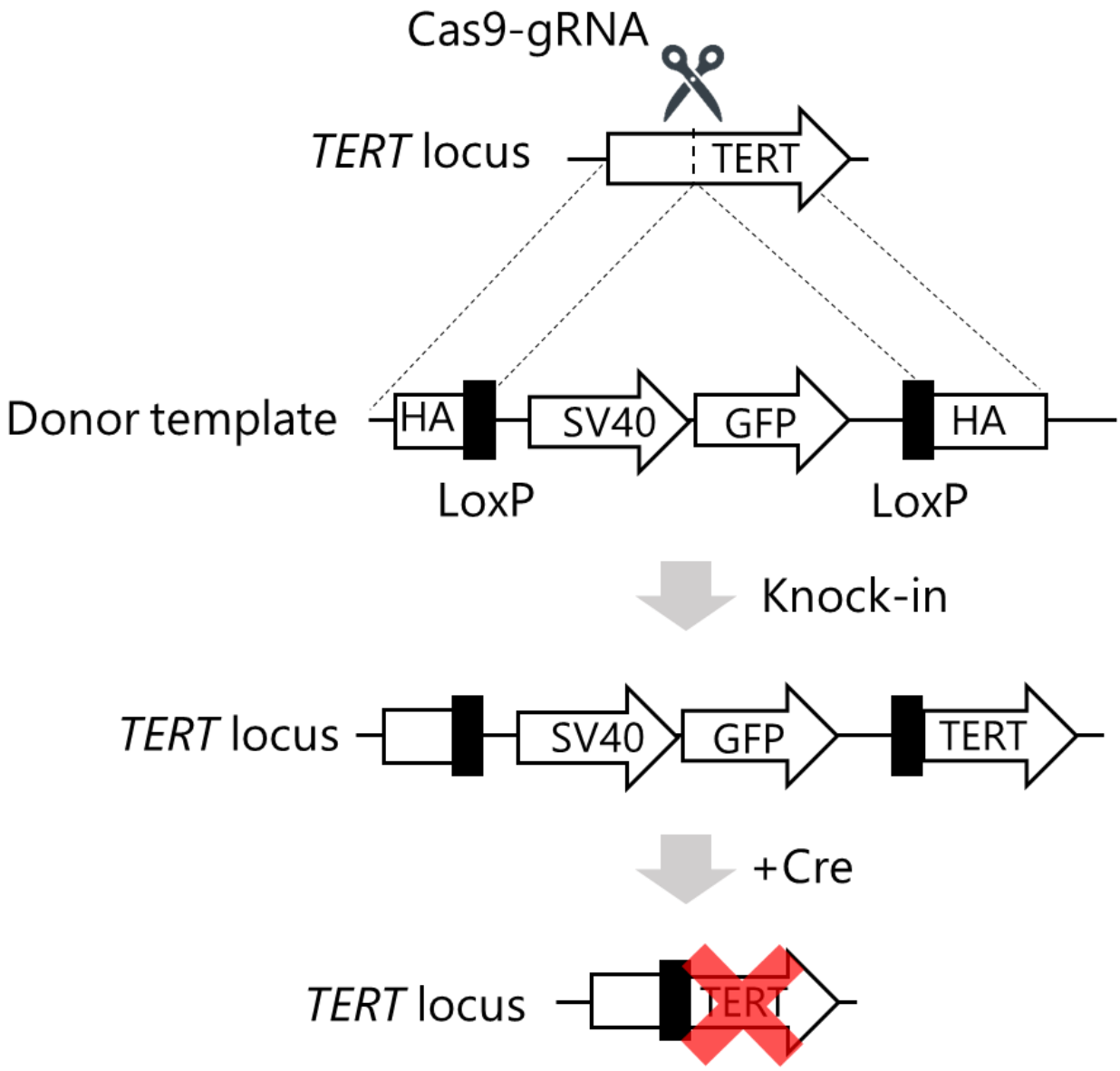

Figure 3.1 Schematic figure for conditional knock out of *TERT* locus.

HA, homology arm

population showing high GFP intensity increased. However, colony PCR for knock-in to *TERT* revealed that no HeLa cell with homozygous knock-in was generated (Fig. 3.2.B). HeLa cells have been reported to have approximately 5 copies of TERT [58], and thus, homozygous knock-in in HeLa cells is more difficult than that in cells with the lower copy number of *TERT*.

Next, I executed knock-in in HEK293T cells, which have been reported to have approximately 2 copies of TERT [58]. Similar to HeLa cells, I transfected the plasmids into HEK293T cells and sorted the cells in flow cytometry by fluorescence intensity of GFP. However, this time, no HEK293Tcell was alive after cell sorting. Thus, I changed sorting method from a cuvette hybrid cell sorter to cell sorter on microfluidic chip, which sorts cell gentler [59]. This change enabled me to isolate HEK293T cells with high GFP expression (Fig. 3.3.A). Nevertheless, colony PCR for knock-in to *TERT* demonstrated that all sorted HEK293T cells were knocked-in heterozygous (Fig. 3.3.B). These results infer that CRISPR/Cas9-based knock-in to *TERT* locus is lethal in HeLa cells and HEK293T cells. To avoid potential stress caused by heterozygous knockout of *TERT*, I used cell lines without genome editing for further study hereafter.

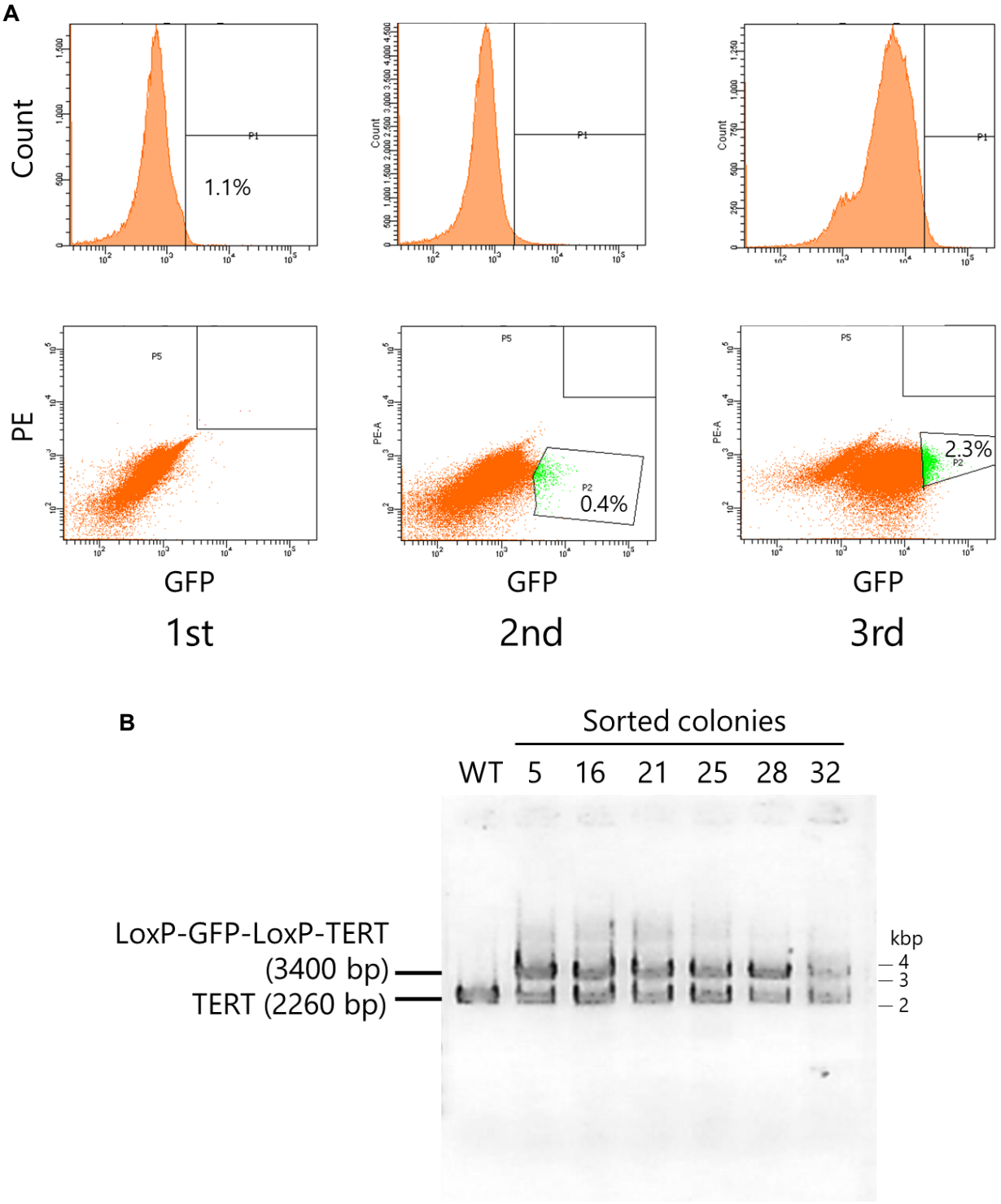

Figure 3.2 Knock-in by CRISPR/Cas9 for conditional knockout of *TERT* did not result in homozygous knock-in in HeLa cells.

A. Distribution of GFP signal in sorted HeLa cells for 3 independent consecutive flow-cytometry. P1, P2, P2 populations were collected in each cell sorting respectively. **B.** Representative image of electrophoresis for colony PCR products.

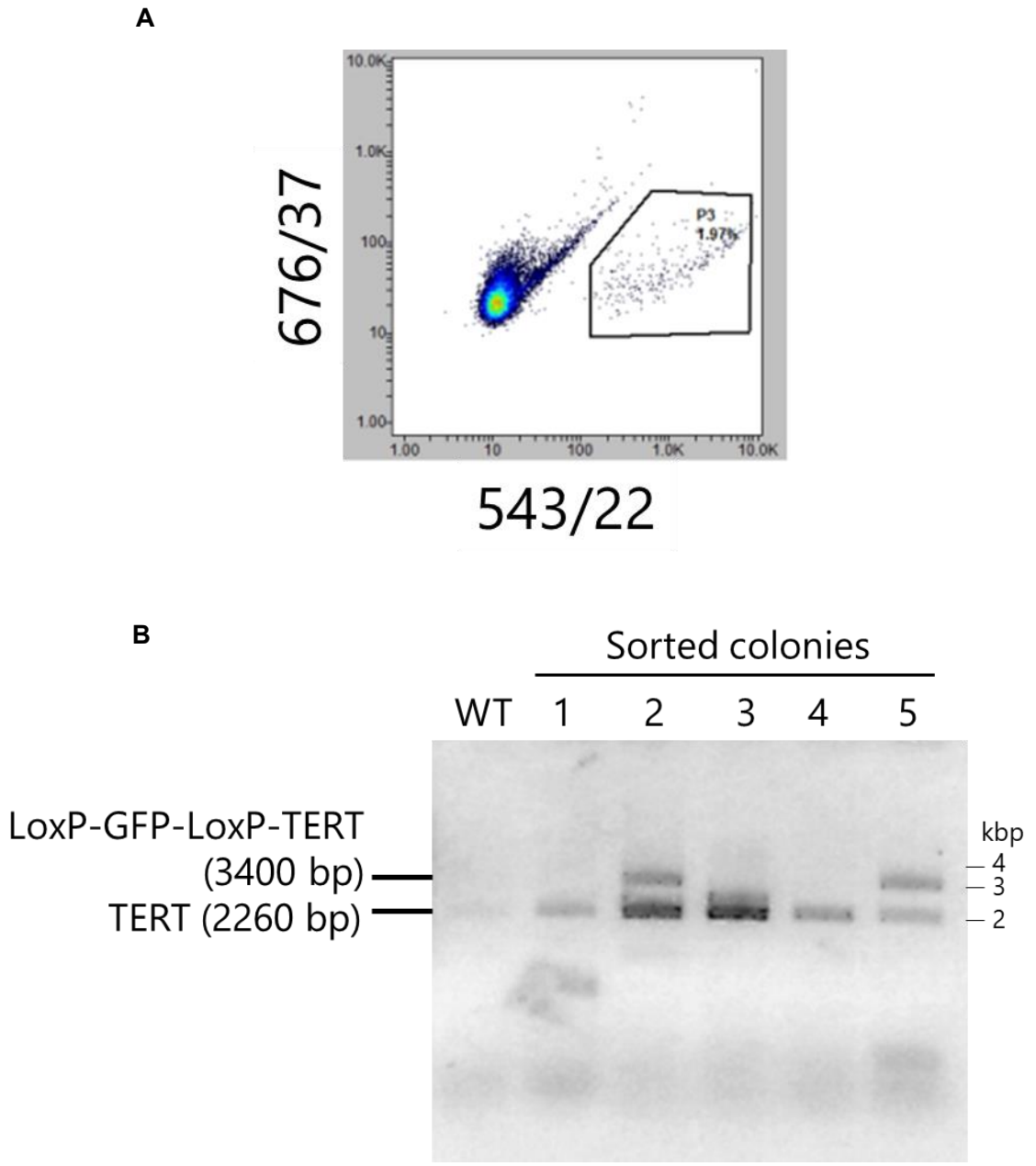

Figure 3.3 Knock-in by CRISPR/Cas9 for conditional knockout of *TERT* did not result in homozygous knock-in in HEK293T cells.

A. Distribution of GFP signal in sorted HEK293T cells. **B.** Representative image of electrophoresis for colony PCR products.

第 3 章

本章の一部については、5 年以内に雑誌等で刊行予定のため、非公開。

CHAPTER 4

DISCUSSION

TERT genome editing

I designed conditional knockout of *TERT* locus by knock-in of GFP for cell sorting and of the target sites of Cre recombinase for conditional knockout after sorting and achieved heterozygous knock-in but did not achieve homozygous knock-in. The lack of homozygous knock-in suggests that homozygous knock-in to *TERT* locus in cancer cells by CRISPR/Cas9 is lethal. This is consistent with the previous studies, which developed the method for knock-in to *TERT* locus. In one of the studies, they adopted the similar strategy for knock-in to *TERT* locus by CRISPR/Cas9 and obtained only heterozygous clones in HeLa and HEK293T cells [57]. Another study for knockout of *TERT* locus by CRISPR/Cas9 also did not succeed in obtaining homozygous clones in HeLa and PANC1 cells [56]. On the other hand, a different group achieved homozygous *TERT* knock-in and knockout clones HCT116 cells by zinc finger nucleases (ZFNs) and in human embryonic stem cells by CRISPR/Cas9 or ZFNs [63, 68]. Previous attempts of CRISPR/Cas9 based genome editing of *TERT* have been limited to target the region between promoter region and exon 6, since they have aimed to knockout of *TERT* or knock-in of epitope tags or fluorescent proteins to the N-terminus of TERT. Therefore, targeting *TERT* at the region after exon 6 might make *TERT* knock-in by CRISPR/Cas9 successful. If double-stranded DNA cleavage of *TERT* locus by nuclease is the reason why no one has succeeded in

acquiring homozygous *TERT* knock-in or knockout clones in cancer cells, genome editing technique without double-stranded DNA cleavage, called base editing can enable to generate homozygous *TERT* knock-in or knockout clones [69]. While base editing requires deep sequencing of genome after introducing other than simple colony PCR performed since it does not change length of target sequence, this requirement would not be a problem because a previous study has established deep sequencing of genome for *TERT* knockout by non-homologous end joining, which changes only several bp of genome [56]. Thus, base editing or genome editing by ZFNs in cancer cells might enable to generate cancer cell lines without endogenous TERT expression.

第 4 章

本章の一部については、5 年以内に雑誌等で刊行予定のため、非公開。

Future perspective

In this thesis, I focused on the non-canonical function of mitochondrial TERT on apoptosis and generate stable cell lines that express full length of TERT fused with mVenus. Actually, TERT has at least 14 alternative splicing variants and most of them lack the domains for telomerase activity [74, 75, 76, 77, 78]. Thus, splicing variants of TERT has also been predicted to play non-canonical

functions. Some of these variants have been highly expressed in cancer cells, and even one of them have localized to mitochondria and nuclear and inhibited apoptosis [79]. The same strategy that I showed in this thesis can be applied to the splicing variant and will elucidate the relationship between its localization and apoptosis inhibition. In addition, to investigate overall regulation of these splicing variants including full-length TERT, knock-in of fluorescent protein to *TERT* locus will be required. I demonstrated that knock-in to *TERT* by CRISPR/Cas9 only produced heterozygous knock-in in cancer cells. Heterozygous *TERT* knock-in might be sufficient for the work of the TERT splicing variants, but homozygous *TERT* knock-in enables to accurately evaluate the regulation of the TERT splicing variants. To achieve homozygous *TERT* knock-in, changing knock-in strategy from CRISPR/Cas9 to different technology such as ZFNs may help. In knock-in of fluorescent protein, the TERT probing method that I developed will be helpful, since most splicing variants retain exon 1 and 2, and the position I inserted mVenus is located at the start of exon 2. My work will be applicable to execute future studies even on alternative splicing variants of TERT.

第４章

本章の一部については、５年以内に雑誌等で刊行予定のため、非公開。

REFERENCES

[1] Smith JS, Chen Q, Yatsunyk LA, *et al*. Rudimentary G-quadruplex-based telomere capping in Saccharomyces cerevisiae. *Nat Struct Mol Biol*. 2011;18(4):478-485.

[2] Ray S, Bandaria JN, Qureshi MH, Yildiz A, Balci H. G-quadruplex formation in telomeres enhances POT1/TPP1 protection against RPA binding. *Proc Natl Acad Sci U S A*. 2014;111(8):2990-2995.

[3] Hayflick L, Moorhead PS. The serial cultivation of human diploid cell strains. *Exp Cell Res.* 1961;25:585-621.

[4] Greider CW, Blackburn EH. Identification of a specific telomere terminal transferase activity in Tetrahymena extracts. *Cell.* 1985;43(2 Pt 1):405-413.

[5] Greider CW, Blackburn EH. The telomere terminal transferase of Tetrahymena is a ribonucleoprotein enzyme with two kinds of primer specificity. *Cell*. 1987;51(6):887-898.

[6] Masutomi K, Kaneko S, Hayashi N, *et al*. Telomerase activity reconstituted in vitro with purified human telomerase reverse transcriptase and human telomerase RNA component. *J Biol Chem.* 2000;275(29):22568-22573.

[7] Yi X, Tesmer VM, Savre-Train I, Shay JW, Wright WE. Both transcriptional and posttranscriptional mechanisms regulate human telomerase template RNA levels. *Mol Cell Biol.* 1999;19(6):3989-3997.

[8] Kim NW, Piatyszek MA, Prowse KR, *et al*. Specific association of human telomerase activity with immortal cells and cancer. *Science*. 1994;266(5193):2011-2015.

[9] Chung J, Khadka P, Chung IK. Nuclear import of hTERT requires a bipartite nuclear localization signal and Akt-mediated phosphorylation. *J Cell Sci.* 2012;125(Pt 11):2684-2697.

[10] Seimiya H, Sawada H, Muramatsu Y, *et al*. Involvement of 14-3-3 proteins in nuclear localization of telomerase. *EMBO J*. 2000;19(11):2652-2661.

[11] Kovalenko OA, Caron MJ, Ulema P, *et al*. A mutant telomerase defective in nuclear-cytoplasmic shuttling fails to immortalize cells and is associated with mitochondrial dysfunction. *Aging Cell*. 2010;9(2):203-219.

[12] Santos JH, Meyer JN, Skorvaga M, Annab LA, Van Houten B. Mitochondrial hTERT exacerbates free-radical-mediated mtDNA damage. *Aging Cell.* 2004;3(6):399-411.

[13] Haendeler J, Hoffmann J, Brandes RP, Zeiher AM, Dimmeler S. Hydrogen peroxide triggers nuclear export of telomerase reverse transcriptase via Src kinase family-dependent phosphorylation of tyrosine 707. *Mol Cell Biol.* 2003;23(13):4598-4610.

[14] Armbruster BN, Banik SS, Guo C, Smith AC, Counter CM. N-terminal domains of the human telomerase catalytic subunit required for enzyme activity in vivo. *Mol Cell Biol*. 2001;21(22):7775-7786.

[15] Yan P, Benhattar J, Seelentag W, Stehle JC, Bosman FT. Immunohistochemical localization of hTERT protein in human tissues. *Histochem Cell Biol*. 2004;121(5):391-397.

[16] Santos JH, Meyer JN, Van Houten B. Mitochondrial localization of telomerase as a determinant for hydrogen peroxide-induced mitochondrial DNA damage and apoptosis. *Hum Mol Genet.* 2006;15(11):1757-1768.

[17] Ahmed S, Passos JF, Birket MJ, *et al*. Telomerase does not counteract telomere shortening but protects mitochondrial function under oxidative stress. *J Cell Sci.* 2008;121(Pt 7):1046-1053.

[18] Singhapol C, Pal D, Czapiewski R, Porika M, Nelson G, Saretzki GC. Mitochondrial telomerase protects cancer cells from nuclear DNA damage and apoptosis. *PLoS One*. 2013;8(1):e52989.

[19] Zhang Z, Yu L, Dai G, *et al*. Telomerase reverse transcriptase promotes chemoresistance by suppressing cisplatin-dependent apoptosis in osteosarcoma cells. *Sci Rep*. 2017;7(1):7070.

[20] Liu K, Hodes RJ, Weng Np. Cutting edge: telomerase activation in human T lymphocytes does not require increase in telomerase reverse transcriptase (hTERT) protein but is associated with hTERT phosphorylation and nuclear translocation. *J Immunol*. 2001;166(8):4826-4830.

[21] Kimura A, Ohmichi M, Kawagoe J, *et al*. Induction of hTERT expression and phosphorylation by estrogen via Akt cascade in human ovarian cancer cell lines. *Oncogene.* 2004;23(26):4505-4515.

[22] Ram R, Uziel O, Eldan O, *et al*. Ionizing radiation up-regulates telomerase activity in cancer cell

lines by post-translational mechanism via ras/phosphatidylinositol 3-kinase/Akt pathway. *Clin Cancer Res*. 2009;15(3):914-923.

[23] Akiyama M, Hideshima T, Hayashi T, *et al*. Nuclear factor-kappaB p65 mediates tumor necrosis factor alpha-induced nuclear translocation of telomerase reverse transcriptase protein. *Cancer Res*. 2003;63(1):18-21.

[24] Jakob S, Schroeder P, Lukosz M, *et al*. Nuclear protein tyrosine phosphatase Shp-2 is one important negative regulator of nuclear export of telomerase reverse transcriptase. *J Biol Chem.* 2008;283(48):33155-33161.

[25] Choi J, Southworth LK, Sarin KY, *et al*. TERT promotes epithelial proliferation through transcriptional control of a Myc- and Wnt-related developmental program. *PLoS Genet.* 2008;4(1):e10.

[26] Koh CM, Khattar E, Leow SC, *et al*. Telomerase regulates MYC-driven oncogenesis independent of its reverse transcriptase activity. *J Clin Invest*. 2015;125(5):2109-2122.

[27] Park JI, Venteicher AS, Hong JY, *et al*. Telomerase modulates Wnt signalling by association with target gene chromatin. *Nature*. 2009;460(7251):66-72.

[28] Ghosh A, Saginc G, Leow SC, *et al*. Telomerase directly regulates NF-κB-dependent transcription. *Nat Cell Biol.* 2012;14(12):1270-1281.

[29] Maida Y, Yasukawa M, Okamoto N, *et al*. Involvement of telomerase reverse transcriptase in heterochromatin maintenance. *Mol Cell Biol.* 2014;34(9):1576-1593.

[30] Masutomi K, Possemato R, Wong JM, *et al*. The telomerase reverse transcriptase regulates chromatin state and DNA damage responses. *Proc Natl Acad Sci U S A*. 2005;102(23):8222-8227.

[31] Lassmann T, Maida Y, Tomaru Y, *et al*. Telomerase reverse transcriptase regulates microRNAs. *Int J Mol Sci*. 2015;16(1):1192-1208.

[32] Haendeler J, Dröse S, Büchner N, *et al*. Mitochondrial telomerase reverse transcriptase binds to and protects mitochondrial DNA and function from damage. *Arterioscler Thromb Vasc Biol.* 2009;29(6):929-935.

[33] Sharma NK, Reyes A, Green P, *et al*. Human telomerase acts as a hTR-independent reverse transcriptase in mitochondria. *Nucleic Acids Res.* 2012;40(2):712-725.

[34] Armstrong L, Saretzki G, Peters H, *et al*. Overexpression of telomerase confers growth advantage, stress resistance, and enhanced differentiation of ESCs toward the hematopoietic lineage. *Stem Cells.* 2005;23(4):516-529.

[35] Indran IR, Hande MP, Pervaiz S. hTERT overexpression alleviates intracellular ROS production, improves mitochondrial function, and inhibits ROS-mediated apoptosis in cancer cells. *Cancer Res*. 2011;71(1):266-276.

[36] Mattiussi M, Tilman G, Lenglez S, Decottignies A. Human telomerase represses ROS-dependent cellular responses to Tumor Necrosis Factor-α without affecting NF-κB activation. *Cell Signal.* 2012;24(3):708-717.

[37] Spilsbury A, Miwa S, Attems J, Saretzki G. The role of telomerase protein TERT in Alzheimer's disease and in tau-related pathology in vitro. *J Neurosci.* 2015;35(4):1659-1674.

[38] Green PD, Sharma NK, Santos JH. Telomerase Impinges on the Cellular Response to Oxidative Stress Through Mitochondrial ROS-Mediated Regulation of Autophagy. *Int J Mol Sci.* 2019;20(6):1509.

[39] Maida Y, Yasukawa M, Furuuchi M, *et al.* An RNA-dependent RNA polymerase formed by TERT and the RMRP RNA. *Nature.* 2009;461(7261):230-235.

[40] Maida Y, Yasukawa M, Masutomi K. De Novo RNA Synthesis by RNA-Dependent RNA Polymerase Activity of Telomerase Reverse Transcriptase. *Mol Cell Biol.* 2016;36(8):1248-1259.

[41] Galluzzi L, Vitale I, Aaronson SA, *et al.* Molecular mechanisms of cell death: recommendations of the Nomenclature Committee on Cell Death 2018. *Cell Death Differ.* 2018;25(3):486-541.

[42] Troyano A, Sancho P, Fernández C, de Blas E, Bernardi P, Aller P. The selection between apoptosis and necrosis is differentially regulated in hydrogen peroxide-treated and glutathione-depleted human promonocytic cells. *Cell Death Differ.* 2003;10(8):889-898.

[43] Teramoto S, Tomita T, Matsui H, Ohga E, Matsuse T, Ouchi Y. Hydrogen peroxide-induced apoptosis and necrosis in human lung fibroblasts: protective roles of glutathione. *Jpn J Pharmacol.* 1999;79(1):33-40.

[44] Jin Y, You L, Kim HJ, Lee HW. Telomerase Reverse Transcriptase Contains a BH3-Like Motif and Interacts with BCL-2 Family Members. *Mol Cells.* 2018;41(7):684-694.

[45] Tochigi M, Inoue T, Suzuki-Karasaki M, Ochiai T, Ra C, Suzuki-Karasaki Y. Hydrogen peroxide induces cell death in human TRAIL-resistant melanoma through intracellular superoxide generation. *Int J Oncol.* 2013;42(3):863-872.

[46] Kowarz E, Löscher D, Marschalek R. Optimized Sleeping Beauty transposons rapidly generate stable transgenic cell lines. *Biotechnol J.* 2015;10(4):647-653.

[47] Mender I, Shay JW. Telomerase Repeated Amplification Protocol (TRAP). *Bio Protoc.* 2015;5(22):e1657.

[48] Schindelin J, Arganda-Carreras I, Frise E, *et al*. Fiji: an open-source platform for biological-image analysis. *Nat Methods*. 2012;9(7):676-682.

[49] Schneider CA, Rasband WS, Eliceiri KW. NIH Image to ImageJ: 25 years of image analysis. *Nat Methods*. 2012;9(7):671-675.

[50] N. Otsu, A Threshold Selection Method from Gray-Level Histograms, *IEEE Transactions on*

Systems, Man, and Cybernetics, 1979;9(1):62-66.

[51] Herbert A (2021). Colocalization ImageJ Plugins. URL http://www.sussex.ac.uk/gdsc/intranet/microscopy/UserSupport/AnalysisProtocol/imagej/colocalisation

[52] R Core Team (2021). R: A language and environment for statistical computing. R Foundation for Statistical Computing, Vienna, Austria. URL https://www.R-project.org/.

[53] Han SK, Lee D, Lee H, *et al*. OASIS 2: online application for survival analysis 2 with features for the analysis of maximal lifespan and healthspan in aging research. *Oncotarget*. 2016;7(35):56147-56152.

[54] Grant Schneider, Eric Chicken and Rachel Becvarik (2021). NSM3: Functions and Datasets to Accompany Hollander, Wolfe, and Chicken - Nonparametric Statistical Methods, Third Edition. R package version 1.16. https://CRAN.R-project.org/package=NSM3

[55] Liu T, Yu H, Ding L, *et al*. Conditional Knockout of Telomerase Reverse Transcriptase in Mesenchymal Cells Impairs Mouse Pulmonary Fibrosis. *PLoS One.* 2015;10(11):e0142547.

[56] Wen L, Zhao C, Song J, *et al*. CRISPR/Cas9-Mediated TERT Disruption in Cancer Cells. *Int J Mol Sci.* 2020;21(2):653.

[57] Xi L, Schmidt JC, Zaug AJ, Ascarrunz DR, Cech TR. A novel two-step genome editing strategy

with CRISPR-Cas9 provides new insights into telomerase action and TERT gene expression. *Genome Biol.* 2015;16:231.

[58] Borah S, Xi L, Zaug AJ, *et al*. Cancer. TERT promoter mutations and telomerase reactivation in urothelial cancer. *Science.* 2015;347(6225):1006-1010.

[59] Wlodkowic D, Darzynkiewicz Z. Rise of the micromachines: microfluidics and the future of cytometry. *Methods Cell Biol*. 2011;102:105-125.

[60] Dunn KW, Kamocka MM, McDonald JH. A practical guide to evaluating colocalization in biological microscopy. *Am J Physiol Cell Physiol.* 2011;300(4):C723-C742.

[61] Van Noorden CJ. The history of Z-VAD-FMK, a tool for understanding the significance of caspase inhibition. *Acta Histochem*. 2001;103(3):241-251.

[62] Singh M, Sharma H, Singh N. Hydrogen peroxide induces apoptosis in HeLa cells through mitochondrial pathway. *Mitochondrion*. 2007;7(6):367-373.

[63] Chiba K, Vogan JM, Wu RA, *et al*. Endogenous Telomerase Reverse Transcriptase N-Terminal Tagging Affects Human Telomerase Function at Telomeres In Vivo. *Mol Cell Biol.* 2017;37(3):e00541-16.

[64] Banik SS, Guo C, Smith AC, *et al*. C-terminal regions of the human telomerase catalytic subunit essential for in vivo enzyme activity. *Mol Cell Biol*. 2002;22(17):6234-6246.

[65] Huard S, Moriarty TJ, Autexier C. The C terminus of the human telomerase reverse transcriptase is a determinant of enzyme processivity. *Nucleic Acids Res*. 2003;31(14):4059-4070.

[66] Nguyen THD, Tam J, Wu RA, *et al*. Cryo-EM structure of substrate-bound human telomerase holoenzyme. *Nature*. 2018;557(7704):190-195.

[67] Ghanim GE, Fountain AJ, van Roon AM, *et al*. Structure of human telomerase holoenzyme with bound telomeric DNA. *Nature*. 2021;593(7859):449-453.

[68] Sexton AN, Regalado SG, Lai CS, *et al*. Genetic and molecular identification of three human TPP1 functions in telomerase action: recruitment, activation, and homeostasis set point regulation. *Genes Dev*. 2014;28(17):1885-1899.

[69] Komor AC, Kim YB, Packer MS, Zuris JA, Liu DR. Programmable editing of a target base in genomic DNA without double-stranded DNA cleavage. *Nature*. 2016;533(7603):420-424.

[70] Kalkavan H, Green DR. MOMP, cell suicide as a BCL-2 family business. *Cell Death Differ*. 2018;25(1):46-55.

[71] Arai K, Masutomi K, Khurts S, Kaneko S, Kobayashi K, Murakami S. Two independent regions of human telomerase reverse transcriptase are important for its oligomerization and telomerase activity. *J Biol Chem*. 2002;277(10):8538-8544.

[72] Mattson MP, Klapper W. Emerging roles for telomerase in neuronal development and apoptosis.

J Neurosci Res. 2001;63(1):1-9.

[73] Chakraborty S, Ghosh U, Bhattacharyya NP, Bhattacharya RK, Roy M. Inhibition of telomerase activity and induction of apoptosis by curcumin in K-562 cells. *Mutat Res*. 2006;596(1-2):81-90.

[74] Kilian A, Bowtell DD, Abud HE, *et al*. Isolation of a candidate human telomerase catalytic subunit gene, which reveals complex splicing patterns in different cell types. *Hum Mol Genet*. 1997;6(12):2011-2019.

[75] Wick M, Zubov D, Hagen G. Genomic organization and promoter characterization of the gene encoding the human telomerase reverse transcriptase (hTERT). *Gene*. 1999;232(1):97-106.

[76] Hisatomi H, Ohyashiki K, Ohyashiki JH, *et al*. Expression profile of a gamma-deletion variant of the human telomerase reverse transcriptase gene. *Neoplasia*. 2003;5(3):193-197.

[77] Saebøe-Larssen S, Fossberg E, Gaudernack G. Characterization of novel alternative splicing sites in human telomerase reverse transcriptase (hTERT): analysis of expression and mutual correlation in mRNA isoforms from normal and tumour tissues. *BMC Mol Biol*. 2006;7:26.

[78] Hrdlicková R, Nehyba J, Bose HR Jr. Alternatively spliced telomerase reverse transcriptase variants lacking telomerase activity stimulate cell proliferation. *Mol Cell Biol*. 2012;32(21):4283-4296.

[79] Listerman I, Sun J, Gazzaniga FS, Lukas JL, Blackburn EH. The major reverse transcriptase-incompetent splice variant of the human telomerase protein inhibits telomerase activity but protects

from apoptosis. *Cancer Res*. 2013;73(9):2817-2828.

[80] Shirasaki Y, Yamagishi M, Suzuki N, *et al*. Real-time single-cell imaging of protein secretion. *Sci Rep*. 2014;4:4736.

[81] Nitta N, Sugimura T, Isozaki A, *et al*. Intelligent Image-Activated Cell Sorting. *Cell*. 2018;175(1):266-276.e13. doi:10.1016/j.cell.2018.08.028

[82] Shin WH, Chung KC. Human telomerase reverse transcriptase positively regulates mitophagy by inhibiting the processing and cytoplasmic release of mitochondrial PINK1. *Cell Death Dis.* 2020;11(6):425.

[83] Haendeler J, Hoffmann J, Diehl JF, *et al*. Antioxidants inhibit nuclear export of telomerase reverse transcriptase and delay replicative senescence of endothelial cells. *Circ Res*. 2004;94(6):768-775.

[84] Kovalenko OA, Kaplunov J, Herbig U, Detoledo S, Azzam EI, Santos JH. Expression of (NES-)hTERT in cancer cells delays cell cycle progression and increases sensitivity to genotoxic stress. *PLoS One*. 2010;5(5):e10812.

ACKNOWLEDGEMENT

I would like to acknowledge a number of people that have been instrumental in my success in completing this dissertation as follows:

・Prof. Sotaro Uemura, who taught me how to think as an independent researcher.

・Dr. Tomohiro Shima, who taught me how to face sincerely to science.

・Dr. Yoshitaka Shirasaki, who encouraged me to pursue my goal inside and outside of research.

・Dr. Ryo Iizuka, who provided detail-oriented significant advice on experiments and writings.

・Ms. Haruka Narita and Mr. Hanjin Liu, who supplied support for experiments and data analysis.

・Dr. Keigo Ikezaki and Dr. Sawako Enoki, who supported confocal microscopy.

・Dr. Saburo Tsuru, who supported flow-cytometry.

・The study was supported by the Japan Society for the Promotion of Science Grant-in-Aid for JSPS Fellows (JP21J10299) to H.E. and by JSPS KAKENHI (18K06147,19H05379 and 21H00387) to T.S.

・Finally, my parents and grandmother, Mr. Norito Ebata and Mrs. Takako Ebata, and Mrs. Yoko Ebata, who supported me throughout my life.